IN-SITU POST-DEPOSITION THERMAL ANNEALING OF CO-EVAPORATED $Cu(InGa)Se_2$ THIN FILMS DEPOSITED AT LOW TEMPERATURES

James D. Wilson, Brian E. McCandless, Robert W. Birkmire, William N. Shafarman
Institute of Energy Conversion, University of Delaware, Newark, DE 19716 U.S.A.

ABSTRACT

The effects of deposition temperature and *in-situ* post-deposition annealing on the microstructure of co-evaporated $Cu(InGa)Se_2$ thin films and on the performance of the resulting solar cell devices have been characterized. Films were deposited at substrate temperatures of 150°C, 300°C and 400°C. Films were also deposited at these temperatures and then annealed *in-situ* at 550°C for 10 minutes. In as-deposited films without annealing, additional XRD reflections that may be due to a polytypic modification of the chalcopyrite phase were observed. Films deposited at 150°C were Se-rich. Post-deposition annealing caused microstructural changes in all films and improved the resulting solar cells. Only films deposited at 400°C, however, yielded high-efficiency devices after post-deposition annealing that were equivalent to devices made from films grown at 550°C. Films originally deposited at 300°C yielded devices after post-deposition annealing with V_{OC} close to that of devices made from films grown at 550°C, despite smaller grain size.

INTRODUCTION

Low temperature deposition of $Cu(InGa)Se_2$ thin films by co-evaporation may be an important part of low-cost manufacturing pathways for $Cu(InGa)Se_2$ solar cells, offering increased flexibility in substrate choice and a reduced energy budget of fabrication. Moreover, alternative synthesis pathways for $Cu(InGa)Se_2$ films that include sputtered precursors, electrodeposition and ink coating are characterized by low or room temperature deposition of film constituents followed by a post-deposition reaction and annealing step. While these synthesis pathways involve distinct chemical reaction steps to obtain the chalcopyrite phase, they may also require annealing and film restructuring, as co-evaporation at low temperature does, in order to yield device quality material.

Decreased substrate temperature (T_{SS}) during deposition by elemental co-evaporation has been shown to result in films with reduced device performance [1,2,3]. It has also been shown, however, that high efficiency devices can be made from $Cu(InGa)Se_2$ films grown at T_{SS}=350°C when deposition is followed by post-deposition thermal annealing (PDA) at T_{SS}=530°C [4]. The total PDA time can be short when the annealing temperature is high. We have previously shown that the performance of devices made from $Cu(InGa)Se_2$ films grown at T_{SS}=400°C followed by in-situ PDA at 550°C for 1-10 minutes was indistinguishable from that of $Cu(InGa)Se_2$ films deposited at T_{SS}=550°C [5].

In addition to reduced device performance, decreased T_{SS} during deposition was also shown to yield films with smaller grains [1,2]. Co-evaporated thin films deposited at T_{SS}=550°C had grains with lateral dimensions on the order of 1 μm while films grown at T_{SS}=400°C had grains with lateral dimensions on the order of 0.1 μm. PDA at T_{SS}=550°C for 10 minutes or more of the films grown at T_{SS}=400°C caused substantial grain growth [5]. Most of the device improvement associated with PDA, however, occurred before substantial grain growth was observed. In particular, we established that PDA improved V_{OC} to its highest value while lateral grain sizes remained on the order of 0.1μm. Subsequent grain growth to ~1 μm, using longer PDA times, had no effect on V_{OC} [5].

This paper presents materials and device analysis for $Cu(InGa)Se_2$ thin films deposited by co-evaporation at T_{SS} from 150°C to 550°C both before and after *in-situ* PDA at T_{SS}=550°C for 10 minutes. Films are characterized using cross-sectional scanning electron microscopy and x-ray diffraction pattern and line profile analysis. Devices are characterized with J-V measurements. The relationship between film structure and solar cell device performance is discussed.

EXPERIMENTAL APPROACH

$Cu(InGa)Se_2$ films were deposited on 1"x1" Mo-coated soda-lime glass (SLG) substrates in a bell-jar system using thermal evaporation from four Knudsen-type elemental sources (copper, indium, gallium and selenium). Source fluxes and T_{SS} were held constant throughout the deposition. Films were grown at T_{SS}=150°C, 300°C, 400°C and 550°C. *In-situ* PDA was performed after deposition was complete at 550°C for 10 minutes, with a 10 minute interval to ramp up from deposition T_{SS} to T_{SS}=550°C. Films were typically deposited with a selenium-to-metal flux ratio (SMR) above 10. For some T_{SS}=150°C depositions, however, the SMR was reduced to between 1 and 2.

All $Cu(InGa)Se_2$ films for this study were 1.5 – 2 μm thick. Their chemical compositions were measured using energy dispersive x-ray spectroscopy (EDS), which yielded Cu/(In+Ga) atomic ratios between 0.8–0.9. The $Cu(InGa)Se_2$ films had Ga/(In+Ga)=0.3, except for a few cases with Ga/(In+Ga)=0.8. The film microstructure was characterized with SEM cross-section images and with XRD 40 kV Cu Kα radiation. The Cu $K\alpha_2$ component of the resulting data was stripped using the Rachinger correction before analysis. The distribution of measured

intensity I(2θ) for the (112) XRD reflection of $Cu(InGa)Se_2$ films was modeled with the Pearson VII function [6,7].

For each 1"x1" $Cu(InGa)Se_2$ film sample, six devices were fabricated with a structure of SLG/Mo/$Cu(InGa)Se_2$/CdS/ZnO/ITO/(Ni/Al grid). No AR coating was used. Devices were characterized by J-V measurements under AM1.5 illumination at 25°C [8]. All reported J-V results are averages of multiple devices from a sample.

RESULTS

Low Temperature Deposition

Thermal coupling between sources and substrates established a practical minimum T_{SS} > 100°C. For films deposited at T_{SS}=150°C and SMR>10, as-deposited films had Se atomic compositions of 56-60%. Reducing the SMR to 1-2 resulted in films with 53-54% Se. Films deposited at T_{SS}=300°C and SMR>10, for comparison, had 50-53% Se.

The measured XRD pattern for all films indicated $Cu(InGa)Se_2$ chalcopyrite structure with the addition of a reflection at 25.7°, as shown in Figure 1, and an apparent peak around 2θ=53.2°, close to the (312)/(116) chalcopyrite peak but not resolved, as seen in Figure 2.

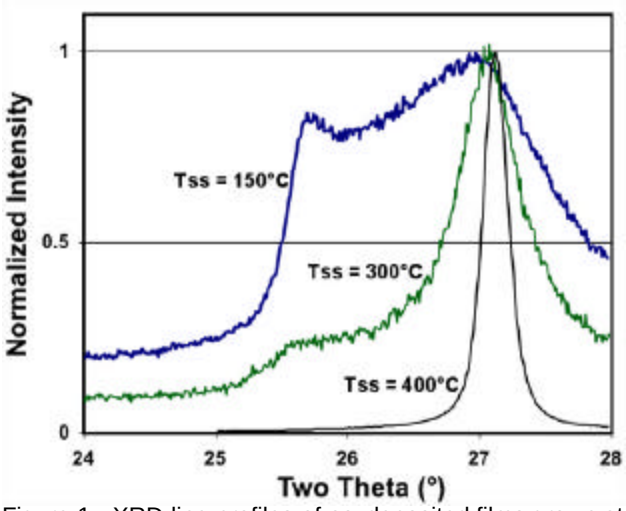

Figure 1. XRD line profiles of as-deposited films grown at T_{SS}=150°C, 300°C and 400°C.

The intensity of the 2θ=25.7° reflection decreased with increasing T_{SS}. At T_{SS}=400°C, it was two or more orders of magnitude less intense than the chalcopyrite (112) peak. For T_{SS}=150°C and 300°C, however, the reflection was much stronger and became comparable in intensity with the chalcopyrite (112) peak. The reflection remained prominent even when the SMR was reduced by an order of magnitude in films deposited at T_{SS}=150°C, as shown in Figure 2.

Additionally, the position of the reflection at an angle just below the (112) reflection shifted with higher Ga/(In+Ga) ratio. With Ga/(In+Ga)=0.3, the chalcopyrite (112) peak was located at 2θ=27.1° and the unidentified reflection was 25.7° and 2) for films with Ga(In+Ga)=0.8, the 2θ values of both peaks increased by approximately 0.5°, as seen in Figure 3.

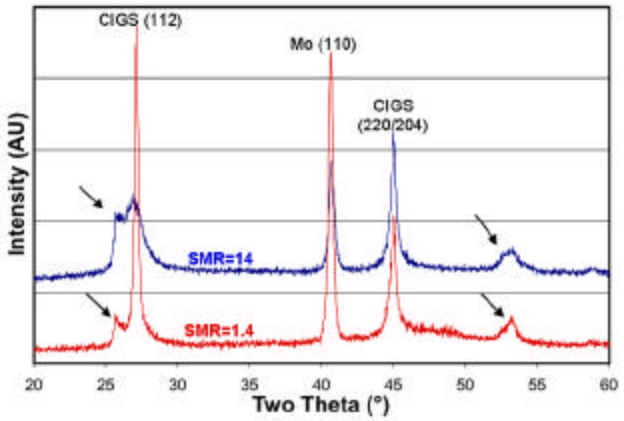

Figure 2. Effect of SMR on XRD pattern of as-deposited films grown at T_{SS}=150°C. Arrows indicate non-chalcopyrite peaks.

The chalcopyrite (312)/(116) reflection is located at 2θ=53.2°. A 2nd order reflection of the same planes producing the 2θ=25.7° peak would be located at 2θ=52.7°, which coincides with the unresolved peak shoulder on the (312)/(116) reflection.

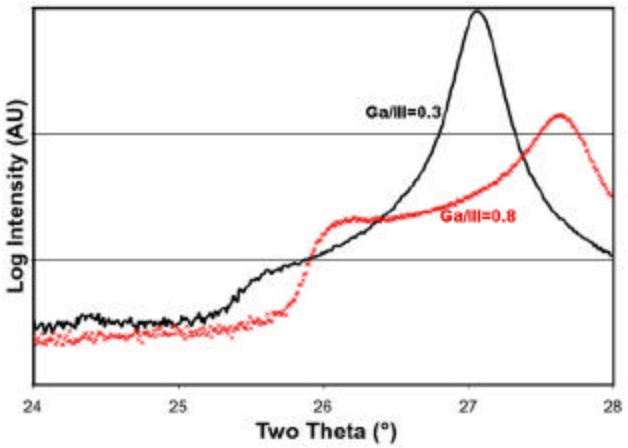

Figure 3. Effect of Ga/(In+Ga) atomic ratio on 2θ values of XRD reflections of as-deposited films grown at T_{SS}=400°C.

With decreasing T_{SS}, the chalcopyrite (112) reflection FWHM increasingly broadened, as shown in Figure 1. The broadening can result from: 1) compositional variation; 2) coherent scattering domain size; 3) non-uniform strain; or 4) stacking faults. Some of these sources can be eliminated. EDS, for example, measures film composition in approximately the top 1 μm of film thickness. Even a doubling of the Ga/(In+Ga) ratio towards the back of the film, however, would only produce a 0.3° increase in the (112) FWHM, whereas films deposited at T_{SS}=300°C have a measured (112) FWHM

around 0.6°, compared to the 0.1° FWHM of the instrument function.

It is theoretically shown [9] and experimentally observed that coherent scattering domain size and strain-induced broadening yield different XRD line profile shapes. Strain broadening results in a Gaussian distribution, while particle size broadening produces a distribution that is similar to a Cauchy (or Lorentzian) function [10]. The measured (112) *I(2q)* of $Cu(InGa)Se_2$ films was modeled with a Pearson VII function, which is a generalization of the Gaussian and Lorentzian distributions [6]. The Pearson VII parameter *m* is indicative of the functional form; $m \to \infty$ converges on the Gaussian function, while $m=1$ reduces to the Lorentzian function. Fitting Pearson VII functions to measured (112) *I(2q)* distributions using *m* as a free fitting parameter yielded best fits with $m<3$. Values of *m* near unity, which are also seen when modeling XRD *I(2q)* from powders, indicate a primarily Lorenztian *I(2q)* distribution which suggests that the observed broadening is primarily a size effect.

In the absence of any evidence of compositional or strain-induced broadening, the Scherrer formula was used to estimate scattering domain sizes, which yielded 5, 10, and 50 nm for films deposited at T_{SS}=150°C, 300°C and 400°C films, respectively.

Post Deposition Annealing

PDA resulted in several changes to the films. The Se concentration in the films grown at T_{SS}=150°C was reduced. All films had 50-53% Se concentrations after PDA. No other change in film composition was measured. Also, the additional XRD reflections at 25.7° and 53° were not observed in any films after PDA. The XRD patterns of the films deposited at T_{SS}=150°C before and after PDA are compared in Figure 4.

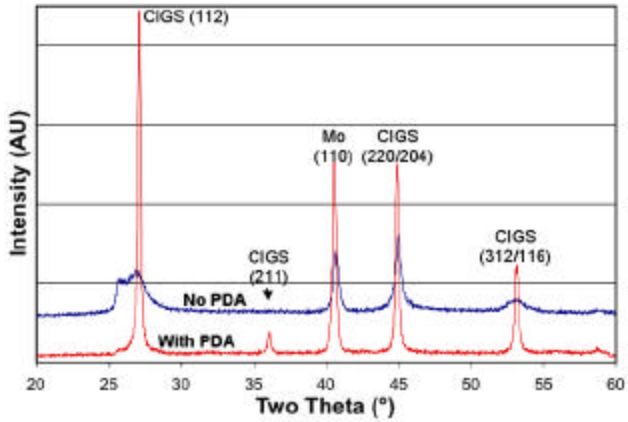

Figure 4. Effect of PDA on XRD patterns of as-deposited films grown at T_{SS}=150°C.

With PDA, films deposited T_{SS}=150°C, 300°C, and 400°C all showed sharpening of the chalcopyrite (112) reflection compared to as-deposited films. For films deposited at T_{SS}=300°C and 400°C and then subjected to PDA, the (112) reflection FWHM sharpened to 0.1°, indistinguishable from that measured on films deposited at T_{SS}=550°C and from the diffractometer instrument function. For films deposited at T_{SS}=150°C the (112) peak FWHM sharpened only to 0.2°. The Scherrer formula yielded domain size estimates of 50 nm, > 0.1 μm and > 0.1 μm for films deposited at T_{SS}=150°C, 300°C and 400°C films with PDA, respectively.

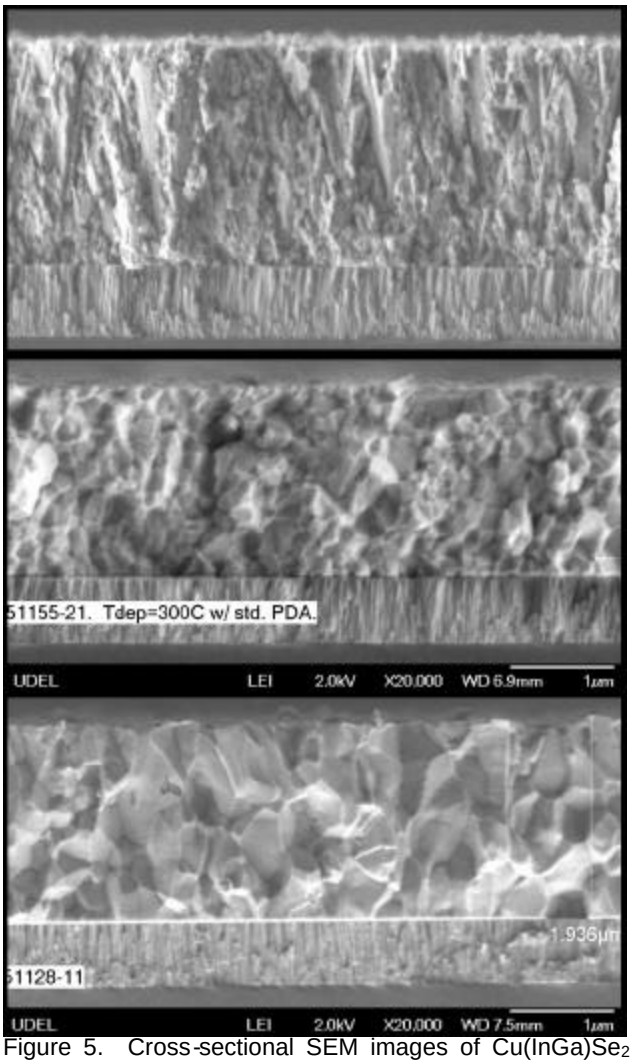

Figure 5. Cross-sectional SEM images of $Cu(InGa)Se_2$ films deposited on Mo/SLG at (a) T_{SS}=150°C, (b) T_{SS}=300°C or (c) T_{SS}=400°C and then annealed at T_{SS}=550°C for 10 minutes. Magnification is the same in all images.

Cross-sectional SEM images after PDA, shown in Figure 5, show the final grain size to be a positive function of the original deposition temperature. Films originally deposited at T_{SS}=300°C and 400°C both appeared to have average grain sizes > 0.1μm, consistent with the absence of broadening seen in the XRD (112) reflection. The film deposited at T_{SS}=150°C has smaller grains which appear of be on the order of 0.1 μm or smaller, also consistent with the Scherrer formula estimate of 50 nm.

The effects of film deposition temperature and PDA on device performance are shown in Table I. For the case of films deposited at T_{SS}=400°C, PDA at 550°C can produce Cu(InGa)Se_2 films that yield $\eta > 15\%$. For the cells made from films deposited at T_{SS}=300°C, PDA improved the performance, but efficiencies were still low compared to devices made from films deposited at either T_{SS}=550°C or to devices made from films deposited at T_{SS}=400°C and then annealed at 550°C.

Table I. Mean device J-V parameters for cells made from Cu(InGa)Se_2 films deposited at different T_{SS} with and without PDA at 550°C for 10 minutes.

Deposition T_{SS} (°C)	V_{OC} (V)	FF (%)	J_{SC} (mA/cm^2)	η (%)
Without PDA				
150	0.17	36	1	0.1
300	0.25	43	13	1.4
400	0.56	66	27	10.0
550	0.64	76	33	15.9
With PDA				
150	0.51	63	20	6.3
300	0.62	66	27	11.0
400	0.65	77	31	15.3

DISCUSSION AND CONCLUSIONS

Three changes characterized as-deposited Cu(InGa)Se_2 films as deposition T_{SS} was decreased. First, at T_{SS}=150°C, at which the saturation pressure for re-evaporation is low, films were Se-rich. Chalcopyrite structure, however, was still observed, even under Se-condensing deposition conditions. Second, the FWHM of XRD reflections broadened and grain size decreased. Third, two new XRD reflections appeared, on the low-angle side of the (112) and (312)/(116) reflections.

The strong intensity of the 2θ=25.7° reflection combined with the absence of any other additional reflections (except for the small peak at ~53° which lies at twice the d-spacing and can be interpreted as a 2nd order reflection of the same planes producing the 25.7° reflection) suggests that an elemental or binary second phase is unlikely. From a mass balance point-of-view, if a substantial fraction of one or two of the film's atomic constituents were tied up in such a second phase, the remaining constituents could not all be accounted for by the chalcopyrite phase and a compositionally balancing third phase would be expected.

The additional x-ray reflection at 2θ=25.7° corresponds to a change in lattice spacing of approximately 5% compared to the chalcopyrite (112) planes. A left shoulder peak with a similar shift in lattice spacing has also been reported in polycrystalline silicon thin films, where it was attributed to a polytypic modification of the silicon crystal structure related to a high density of planar faults [11]. We propose that the observed 25.7° reflection is an analogous modification of or ordered defect within the chalcopyrite phase in Cu(InGa)Se_2.

PDA caused substantial change in the structure of all films as indicated XRD line sharpening and x-SEM images. The films after PDA, however, had smaller grains with lower growth T_{SS}.

From a device perspective, PDA improved the resulting solar cell devices compared to devices made from as-deposited films but only devices made from films deposited at T_{SS}=400°C had efficiencies >15%, comparable to devices made from films deposited at T_{SS}=550°C. For cells made from films grown at T_{SS}=300°C, V_{OC} reached a value comparable to that obtained on devices made from films grown at T_{SS}=550°C, while J_{SC} and FF were inferior.

It is notable that the different film structures observed in Figures 5(b) and 5(c) both yielded devices with comparable V_{OC}. This is consistent with our previous result that PDA improves V_{OC} to its highest value while lateral grain sizes remain on the order of 0.1 μm [5].

ACKNOWLEDGEMENTS

The authors gratefully acknowledge the technical assistance of Josh Cadoret and Kevin Hart.

This material is based upon work supported by the Department of Energy under Award Number DE-FC36-08GO18019.

This report was prepared as an account of work sponsored by an agency of the United States Government. Neither the United States Government nor any agency thereof, nor any of their employees, makes any warranty, express or implied, or assumes any legal liability or responsibility for the accuracy, completeness, or usefulness of any information, apparatus, product, or process disclosed, or represents that its use would not infringe privately owned rights. Reference herein to any specific commercial product, process, or service by trade name, trademark, manufacturer, or otherwise does not necessarily constitute or imply its endorsement, recommendation, or favoring by the United States Government or any agency thereof. The views and opinions of authors expressed herein do not necessarily state or reflect those of the United States Government or any agency thereof.

REFERENCES

[1] W. Shafarman and J. Zhu, "Effect of Substrate Temperature and Deposition Profile on Evaporated Cu(InGa)Se_2 Films and Devices*", Thin Solid Films* **361-362**, p. 473 (2000).

[2] W. Shafarman and J. Zhu, "Effect of Grain Size, Morphology and Deposition Temperature on Cu(InGa)Se_2 Solar Cells*", Mat. Res. Soc. Symp. Proc*. **668**, p. H2.3.1 (2001).

[3] M. Lammer, R. Kniese and M. Powalla, “In-line Deposited Cu(In,Ga)Se_2 Solar Cells: Influence of Deposition Temperature and Na Co-evaporation on Carrier Collection”, *Thin Solid Films* **451-452**, p. 175 (2004).

[4] T. Wada, S. Nishiwaki, Y. Hashimoto and T. Negami, “Physical Vapor Deposition of Cu(In,Ga)Se_2 Films for Industrial Application”, *Mat. Res. Soc. Symp. Proc***. 668**, p. H2.1.1 (2001).

[5] J. Wilson, R. Birkmire and W. Shafarman, “In-situ Annealing of Cu(InGa)Se_2 Films Grown by Elemental Co-evaporation,” *Proc. 33rd IEEE Photovoltaic Specialists Conf., May12-16, San Diego* (2008).

[6] M. Hall, V. Veeraraghavan, H. Rubin and P. Winchell, “The Approximation of Symmetric X-ray Peaks by Pearson Type VII Distributions,” *J. Appl. Cryst*. **10**, p. 66 (1977).

[7] R. Young and D. Wiles, “Profile Shape Functions in Rietveld Refinements,” *J. Appl. Cryst* **15**, p. 430 (1982).

[8] W. Shafarman, R. Klenk and B. McCandless, “Device and material characterization of Cu(InGa)Se2 solar cells with increasing band gap,” *J. Appl. Phys.* **79**, p.7324 (1996).

[9] C. Barrett and T. B. Massalski, Structure of Metals, 3rd Edition, Pergammon (1980) p. 451.

[10] B. Warren, “X-ray Studies of Deformed Metals,” *Prog. Metal Phys.* **8**, p.147 (1959).

[11] M. Hendriks, S. Radelaar, A. Beers, and J. Bloem, “Additonal X-ray and Electron Diffraction Peaks of Polycrystalline Silicon Films,” *Thin Solid Films* **113**, 59 (1984).